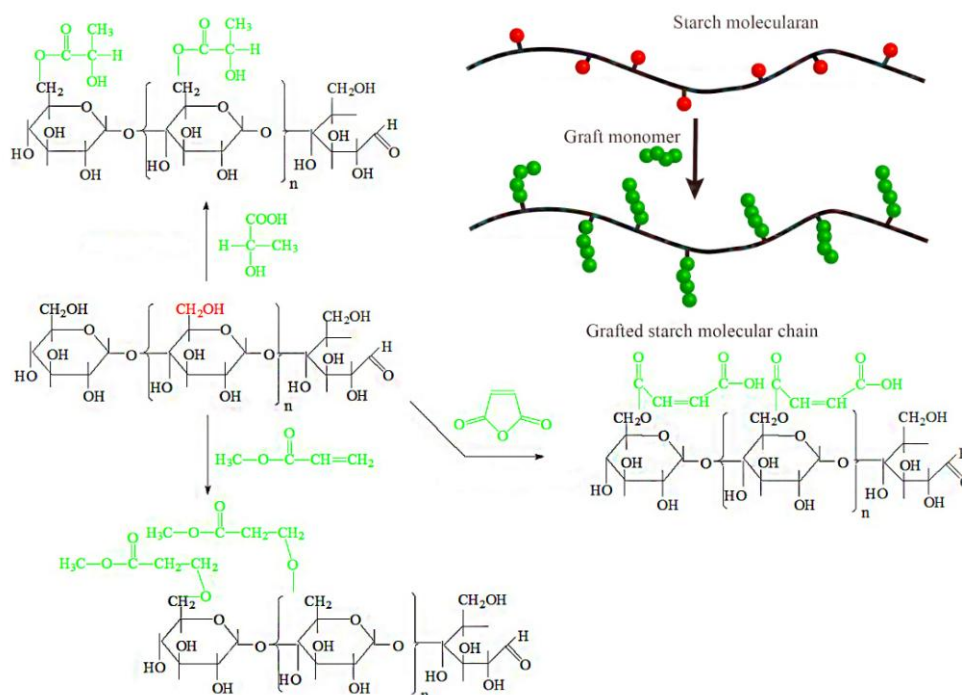




43 hydroxy groups on the starch molecules chain [8,9]. To do this, most strategies have focused on  
 44 the grafting of highly reactive hydrophobic functional groups onto the starch polymeric backbone  
 45 [10-12]. The grafted functional groups could react with the hydroxyl groups of starch  
 46 macromolecules to form covalent bonds, providing better control of phase size and improved  
 47 interfacial adhesion. Additionally, Sagar [13] believed that modification of starch could increase  
 48 the length of the starch side chain, which enhanced thermoplastic and hydrophobic characteristics,  
 49 and that the hydrophobic function group in the starch structure could play the role of  
 50 plasticization.

51 Hydrophobic groups graft starches were usually produced by wet method, organic solvent  
 52 method [14], reactive extrusion method [15] and microwave-assisted method [16,17]. The wet  
 53 method is performed in an aqueous solution, so the reaction is homogeneous and environmentally  
 54 friendly. However, the hydrolytic side reaction of anhydride cannot be ignored in this process. The  
 55 organic solvent method offers homogeneous reaction, but has a low degree of substitution of  
 56 products, high output cost, and causes environmental pollution. The reactive extrusion method  
 57 requires the addition of a plasticizer, and this will make the starch undergo plasticization, changing  
 58 the granular structure of the starch. The microwave-assisted method is not suitable for large-scale  
 59 industrial production, as the process is relatively complex and requires significant energy  
 60 consumption.



61

### 62 **Fig.1 In-situ solid phase polymerization of corn starch and hydrophobic groups**

63

64

65

66

67

68

69

70

Considering the limitations of the current technological methods used to graft hydrophobic  
 groups to starch, the objective of this investigation was to produce hydrophobic groups grafted to  
 starches by an in-situ solid phase polymerization method. In this process, dry starch, reaction  
 monomers, and a catalyst are mixed in a closed hydrothermal reactor, and in-situ polymerization  
 of the starch and reaction monomers is initiated under pressure at 80 °C (Fig.1). This approach is a  
 promising green production method with many advantages. First, this process uses a reaction  
 temperature that is lower than traditional methods and produces less by-products and degradation  
 products. Second, the reacting monomer is in complete contact with the starch, so that the reaction

71 is efficient. Third, the polycondensation reaction was stable and could be scaled to the industrial  
72 level. Four, the reaction is performed in the presence of solvents, for a more environmentally  
73 friendly condensation process. Furthermore, the pressure will be generated automatically in the  
74 reactor when the temperature reaches a certain range, to accelerate the reaction rate. Therefore, the  
75 proposed process of in-situ solid phase polymerization of starch and reaction monomers is a new,  
76 facile, and effective way to improve the interfacial compatibility of hydrophilic starch and  
77 hydrophobic polymer. Anhydrides, carboxylic acids and acrylate compounds were commonly used  
78 in hydrophobic modification of starch and interfacial modification of starch/polymer matrix  
79 composites [18-21]. Among them, maleic anhydride (MAH), lactic acid (LA) and methyl acrylate  
80 (MA) were most commonly used. This was mainly due to that MAH and LA has carboxyl groups  
81 and MA contains free radical polymerization of C=C, which can react with hydroxyl groups in  
82 starch. Therefore, to test this in-situ solid phase polymerization method, maleic anhydride, lactic  
83 acid, and methyl acrylate were used as graft monomers to prepare hydrophobically-modified  
84 starch. The grafting effect and hydrophobicity modification were then compared for the three  
85 kinds of grafting monomers. So, as to improve the application range of starch in the field of  
86 thermoplastic starch and starch/polymer composites.

## 87 **2. Materials and methods**

### 88 **2.1 Materials**

89 Corn starch was obtained from Dacheng Corn Development Co. Ltd (Changchun, Jilin,  
90 China), and dried in a vacuum drying oven of 50 °C for 48 h to eliminate moisture before use.  
91 Methyl acrylate was obtained from Tianjin Kwangfu Fine Chemical Industry Research Institute  
92 (Tianjin, China). Lactic acid and stannous octoate were supplied by Sinopharm Chemical Reagent  
93 Co., Ltd. Maleic anhydride, acetone, and ammonium persulfate were purchased from Tianjin  
94 Kemiou Chemical Reagent Co., Ltd. (Tianjin, China). All chemicals were AR grade.

### 95 **2.2 Preparation of hydrophobically modified starch**

96 30 g corn starch was added into a hydrothermal reactor, together with 4.5 g grafting monomer  
97 and 0.9 g stannous octanoate catalyzer, mixed, and ground evenly. The hydrothermal reactor was  
98 sealed and placed in an oven at 80 °C for in-situ solid phase polymerization. Heating was stopped  
99 after 2 h. When the reacted starches were cooled to room temperature, acetone was added to the  
100 mixture. The mixture was stirred and then subjected to suction filtration. Finally, the mixture was  
101 washed three times with acetone and dried in an oven at 55 °C until constant weight was achieved.

102 At the same time, in order to compare the grafting effect of in-situ solid phase polymerization,  
103 the graft copolymerization of starch was carried out by aqueous phase polymerization method and  
104 organic solvent polymerization method. Deionized water as a solvent in aqueous phase  
105 polymerization, and tetrahydrofuran was selected by organic solvent polymerization. Starch and  
106 solvents were mixed into starch emulsion according to the mass of 1/9, and protection of nitrogen  
107 in the reaction system. The reaction temperature, reaction time, catalyzer and the treatment of  
108 grafted starches were consistent with in-situ solid phase polymerization.

### 109 **2.3 Properties and characterization**

#### 110 **2.3.1 Fourier transforms infrared spectroscopy (FT-IR) analysis**

111 In order to characterize the chemical changes in the grafted starch, the samples were tabletted  
112 with KBr and subjected to FTIR (IRAffinity-1, Shimadzu). To completely remove the moisture,  
113 the native starch and hydrophobic group grafted starch materials were further dried in a muffle  
114 oven (at 50 °C) for 48 h. The tested samples were obtained after grinding fully using a weight

115 ratio of sample: KBr of 1:100. The FTIR curves for the samples were obtained in a range of  
116 400-4000  $\text{cm}^{-1}$ .

### 117 2.3.2 X-ray photoelectron spectroscopy (XPS) analysis

118 XPS measurements were performed at room temperature with monochromatic AlK $\alpha$   
119 radiation (1486.6eV) using a K-Alpha X-ray photoelectron spectrometer (supplied by Thermo  
120 Fisher Scientific Co., Ltd). The X-ray beam was a 100 W, 200 mm-diameter beam raster over a 2  
121 mm by 0.4 mm area on the sample. A high-energy photoemission spectrum was collected using  
122 pass energy of 50 eV and resolution of 0.1 eV. For the Ag $3d_{5/2}$  line, these conditions produced an  
123 FWHM of 0.80 eV.

### 124 2.3.3 Determination of grafting ratio

125 First, 1.00 g of dry grafted starch was weighed and placed in a 250 mL conical flask. Next,  
126 10 mL of 75% ethanol solution in deionized water was added into the flask, followed by the  
127 addition of 10mL of 0.5mol/L aqueous sodium hydroxide solution. The stoppered conical flask  
128 was agitated, warmed to 30  $^{\circ}\text{C}$ , and stirred for 1 h. The excess alkali was then back-titrated with a  
129 standard 0.5 mol/L aqueous hydrochloric acid solution. A blank titration was performed using  
130 native, un-modified starch. The grafting ratio (GR) was calculated as follows:

$$131 \quad W = \frac{Mc(V_0 - V_1)}{1000 \times nm} \times 100\%$$

$$132 \quad GR = \frac{162W}{M \times (100 - W)} \times 100\%$$

133 Where  $W$  is the substitution degree of the hydrophobic group, %;  $M$  is the molecular weight  
134 of the graft monomer;  $c$  is the concentration of the aqueous hydrochloric acid solution, mol/L;  $V_0$   
135 is the consumed volume of aqueous hydrochloric acid solution by the blank sample, mL;  $V_1$  is the  
136 consumed volume of aqueous hydrochloric acid solution by the grafted starch sample, mL;  $n$  is the  
137 number of hydrophobic groups from the grafted monomer;  $m$  is the mass of the sample, g.

### 138 2.3.4 Contact angle measurement

139 The native starch and grafted starches were weighed, mixed and pressed into a pie sample of  
140 1.5cm diameter with a press machine which pressure was 20 MPa. An optical contact angle  
141 measurement instrument (Data Physics OCA20) was used to measure the contact angle of samples,  
142 using distilled water as the test solution. For each measurement, 4  $\mu\text{L}$  liquid in a microsyringe was  
143 dripped on to the surface of the samples, and the contact angle values were measured until 0  $^{\circ}$ .

### 144 2.3.5 Determination of water absorption

145 To determine the water absorption of the grafted starches, 4.0 g native starch and grafted  
146 starches (dry base) were separately placed in glass dishes that contained a set amount of water.  
147 Over the test period the weight of each sample was measured every 12 h. The water absorption  
148 was calculated as follows:

$$149 \quad \text{water absorption} = \frac{W_t - W_0}{W_0} \times 100\%$$

150 Where  $W_t$  was the weight of the sample after water absorption for  $t$  hours and  $W_0$  was the  
151 weight of sample when it reached drying constant weight.

### 152 2.3.6 Gel Permeation Chromatography (GPC) measurement

153 The molecular weight of native starch, MAH-g-starch, LA-g-starch and MA-g-starch were  
154 tested with a gel permeation chromatograph system (Viscotek TDA305max, Malvern Co., Ltd).

155 The solvent was dimethyl sulfoxide (DMSO)+20 mmol LiBr, the column set was IGuard + 1 x I-H,  
156 the flow rate was 0.500 mL/min, the injection volume was 100 uL, and the detector and column  
157 temperature were 50 °C.

### 158 **2.3.7 Hot paste viscosity testing**

159 The hot paste viscosities of the native starch and grafted starches were measured with a  
160 Rotational Viscometer (Shanghai Pingxuan Scientific Instrument Co. Ltd, China). Starch slurry  
161 with a mass percentage of 6% was prepared by dispersing starch (4.2 g dry basis) in 65.8 g  
162 distilled water and then heating in a 95 °C constant-temperature water bath. The rotational  
163 viscometer was connected to the thermostat and gradually increased to 95 °C, and then maintained  
164 for 15 min. The viscosity value was recorded when the viscometer became stable.

### 165 **2.3.8 Scanning electron microscope (SEM) analysis**

166 The morphology of the native starch and grafted starches was determined with a scanning  
167 electron microscope (QUANTA 200, FEI), operating at an acceleration voltage of 20 kV. Starch  
168 granules were mounted on circular aluminum stubs with double-sided adhesive tape and coated  
169 with gold before testing.

### 170 **2.3.9 X-ray diffraction (XRD) analysis**

171 The native starch and grafted starches samples were further dried in a vacuum oven at 50 °C  
172 for 48 h to remove the remaining moisture. The crystallinity index of the samples was measured  
173 by an X-ray diffractometer (XD-2, Beijing's General Instrument Co., LTD) with Cu target at 36  
174 Kv and 20 mA. Samples were tested in the angular range of  $2\theta = 5^{\circ}$ – $40^{\circ}$  with a scanning rate of  
175 4 °/min.

### 176 **2.3.10 Thermogravimetric (TGA) analysis**

177 TGA measurements of native starch and grafted starch samples were made with a 209 F3  
178 TGA instrument (NETZSCH Co., Germany). About 5 mg of dried sample powders were placed in  
179 a platinum crucible and heated from 25 °C to 800 °C at the rate of 10 °C/min. Dynamic carrier  
180 nitrogen gas flowed at a rate of 30 mL/min. Thermogravimetric (TG) and derivative  
181 thermogravimetric (DTG) data were obtained for each sample.

### 182 **2.3.11 Differential scanning calorimeter (DSC)**

183 The gelatinization temperature of NS, DS and ATDS were studied by using a Differential  
184 Scanning Calorimeter (NETZSCH D204, Germany) as described by Sandhu and Singh [22].  
185 Starch (3.5 mg, dry weight) was loaded into an aluminum pan and distilled water was added with  
186 a microsyringe to achieve a starch-water suspension containing 70 g/100 g water. Samples were  
187 hermetically sealed and allowed to stand for 1 h at room temperature before heating in DSC. The  
188 DSC analyzer was calibrated using indium and an empty aluminum pan was used as reference.  
189 Sample pans were heated at a rate of 5 °C/min from 30 to 200 °C.

## 190 **3. Results and Discussion**

### 191 **3.1 Graft reaction confirmation**

192 [Fig.1](#) depicts the graft reaction between hydrophobic monomers and native corn starch. As  
193 showing, successful reaction adds a new functional group (C=O) to the starch molecule. FTIR  
194 analysis of native starch and grafted starches was performed to verify that the graft reaction  
195 occurred and to investigate the resulting chemical changes. The results of this analysis are shown  
196 in [Fig.2](#).



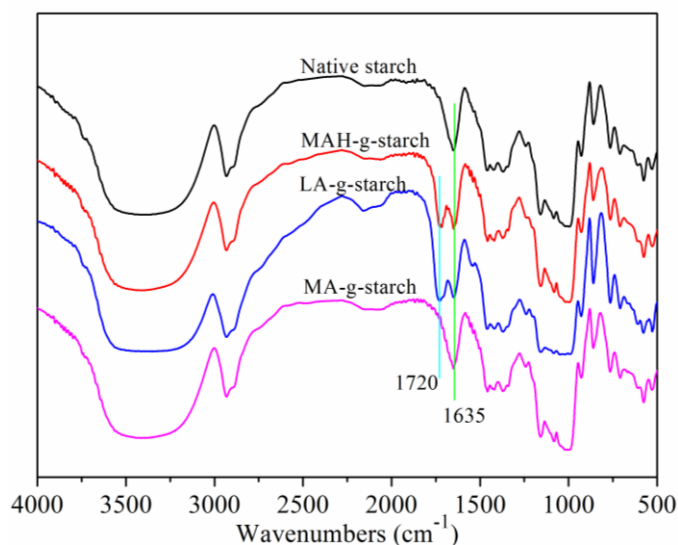
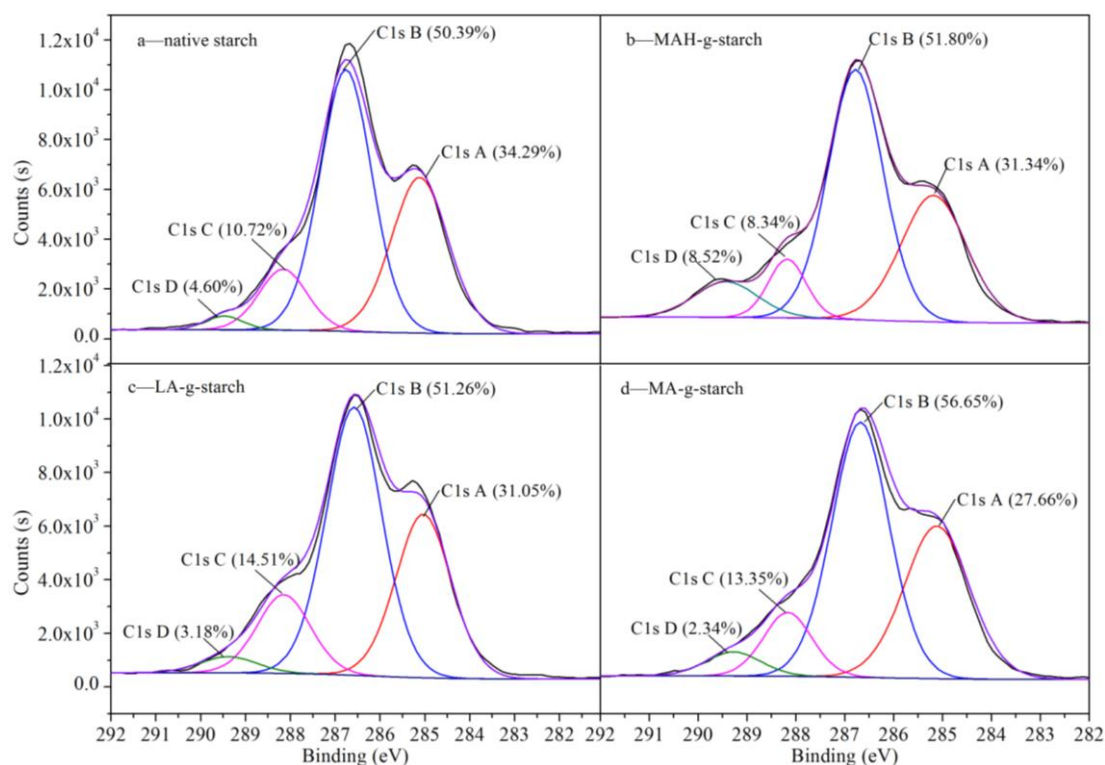


**Fig.2 Infrared spectrum of native starch and grafted starches**

The basic compositional unit of native corn starch is D-anhydroglucose, with C2 and C3-linked secondary hydroxyls as the main characteristic functional groups, a C6-linked primary hydroxyl, and D-pyranose ring structure [23]. The position of the absorption peaks in the infrared spectrum for these main structures are shown in Fig.2: the characteristic peak centered at 3310  $\text{cm}^{-1}$  corresponds to O-H stretching and vibration of the hydrogen bond association, 2930  $\text{cm}^{-1}$  corresponds to C-H asymmetrical stretching and vibration, 1635  $\text{cm}^{-1}$  arises from the water that is tightly bound to the starch, 1152  $\text{cm}^{-1}$  is from C-O-C asymmetrical stretching and vibration, 1080  $\text{cm}^{-1}$  corresponds to D-glucopyranose and hydroxyl-linked C-O stretching and vibration, and 925  $\text{cm}^{-1}$  is due to glucosidic bond vibration [24]. The infrared spectra for the grafted starches include all of the above characteristic absorption peaks, but also contain a C=O absorption peak at 1720  $\text{cm}^{-1}$  [25,26]. Following the reaction of the starch with hydrophobic monomers, the un-reacted hydrophobic monomers and homopolymer was removed by the acetone wash. It could be confirmed that the C=O came from grafted starches according to the positions which appeared, which verified that the graft reaction had occurred between the native starch and grafting monomer.

To further validate that the grafting reaction had occurred, the samples were subjected to X-ray photoelectron spectroscopy (XPS) to establish the binding modes of C in the samples, the results are shown in Fig.3 and Table 1. Compared with native starch, the relative concentration of C-containing groups with binding energy between 284.9 eV and 289.0 eV was significantly different in the grafted starch samples. Comparing the XPS spectrum of native starch (Fig.3a) to the spectra of MAH-g-starch (Fig.3b), LA-g-starch (Fig.3c) and MA-g-starch (Fig.3d) shows that the intensity of peak at 284.9 eV was decreased, which was attributed to the presence of more C-C/C-H groups. At the same time, the intensity of the peak at 286.1 eV was decreased, which represented the presence of C-O groups. And seeing from the results in Fig.3, the amount of C-O in the grafted starches was higher than that in the native starch, which was attributed to the high incidence of grafted molecular chains in the grafted starch material. The intensity of the 287.6 eV peak was also changed, which represented the presence of C-C=O groups. In addition, the intensity of the 289.0 eV peak for the modified starch was also changed, which was attributed to the abundance of O=C-O groups. The chemical environmental changes indicated that the corn

228 starch had reacted with the hydrophobic monomer through in-situ solid phase polymerization, in  
 229 which the C-O(H) bond was broken and carbonyl groups (C=O) were generated. The results of the  
 230 relative content of each chemical structure indicated that there was a different in the content of  
 231 C=O in three kinds of grafted starches. The content of C=O in native starch was 15.32%, after the  
 232 treatment, the C=O content increased to 16.86% in MAH-g-starch, 17.69% for LA-g-starch, and  
 233 15.69% for MA-g-starch. This difference in the three treated starches may be due to different  
 234 reaction efficiencies, resulting in differences in the grafting ratio. To verify these differences, the  
 235 grafting ratio was tested for the three kinds of graft starches.



236

237 **Fig.3 The binding modes of C in native starch and grafted starches**

237

### 238 3.2 The grafting ratio for different hydrophobic monomers

238

239 The reaction variable of the in-situ solid phase polymerization reaction between native starch and  
 240 hydrophobic monomer was directly related to the variety of hydrophobic monomer, and inevitably  
 241 leads to the difference in the grafting ratio. At the same time, the graft copolymerization of starch  
 242 was carried out by aqueous phase polymerization method and organic solvent polymerization  
 243 method, and the grafting ratio has been tested, the results are shown in Table 1.

244

**Table 1 Grafting ratio of three kinds of grafted starches**

Grafted starches	In-situ solid phase polymerization		Aqueous phase polymerization		Organic solvent polymerization	
	W (%)	GR (%)	W (%)	GR (%)	W (%)	GR (%)
MAH-g-starch	3.79	6.50	1.27	2.13	3.58	6.14
LA-g-starch	6.47	12.45	3.06	5.68	5.91	11.31
MA-g-starch	0.33	0.57	0.12	0.23	0.32	0.60

245

246

247

As shown in Table 1, compared with in-situ solid phase polymerization, the degree of substitution and grafting ratio of aqueous phase polymerization were relatively small. This was due to the presence of hydrolytic side reactions in aqueous phase, resulting in smaller grafting

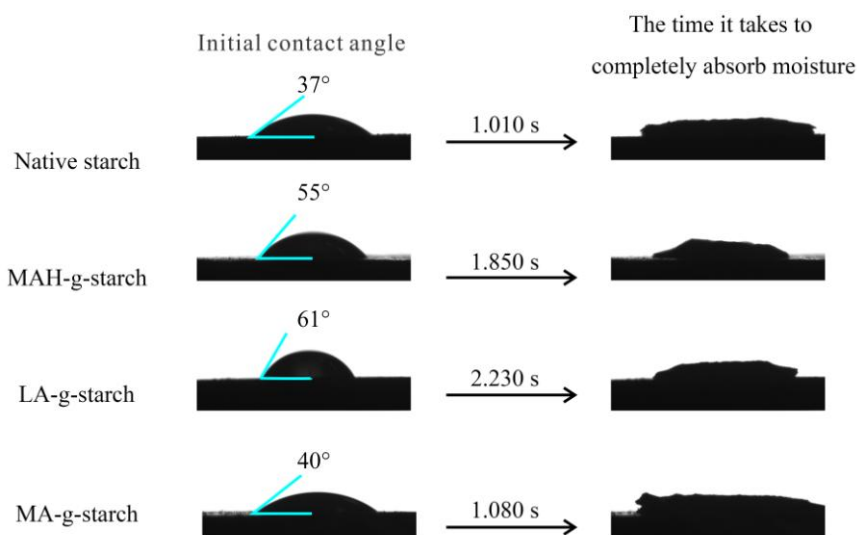
248 ratio. The degree of substitution and grafting ratio of grafted starches prepared by organic solvent  
249 polymerization was also smaller than those of in-situ solid phase polymerization. It was indicated  
250 that starch and graft monomers had the highest reaction efficiency through in-situ solid phase  
251 polymerization. The reaction efficiency of different graft monomers was also different. Moreover,  
252 the change trend of degree of substitution and grafting ratio of the grafted starches prepared by  
253 different grafting methods were the same.

254 With the in-situ solid phase polymerization, the grafting ratio of MAH-g-starch was 6.50%,  
255 that of LA-g-starch was 12.45%, and MA-g-starch was 0.57%. The results show that the  
256 efficiency of in-situ solid phase polymerization for lactic acid and starch was the highest under  
257 these conditions. The XPS analysis showed that the C=O content of LA-g-starch was the highest  
258 and that of MA-g-starch was the smallest. The in-situ solid phase polymerization of lactic acid and  
259 maleic anhydride with starch occurred as esterification, while methyl acrylate occurred as radical  
260 polymerization. The reaction conditions required for radical polymerization are more stringent,  
261 resulting in the lowest grafting ratio for MA-g-starch. Lactic acid is a liquid that can penetrate into  
262 the starch well before the reaction, increasing the chance of contact with hydroxyl groups on the  
263 starch. In contrast, maleic anhydride is solid, and does not penetrate into the starch to react with  
264 hydroxyl until the temperature exceeds its melting point (52.8 °C). Additionally, maleic anhydride  
265 needs to open the acid anhydride to react with hydroxyl groups. These two reasons cause the  
266 grafting ratio of the LA-g-starch to be significantly greater than that of the MAH-g-starch.

### 267 **3.3 Hydrophobic property of grafted starches**

268 The molecular chain of the native starch contains many hydrophilic hydroxyl groups, and the  
269 grafting of hydrophobic groups onto the native starch would improve the hydrophobicity of the  
270 starch. The contact angle (CA) of water on a surface is the angle formed by a tangent line from the  
271 water droplet to the solid surface, and is an indication of the relative hydrophobic character of the  
272 sample surface. Generally speaking, the larger the CA, the higher the hydrophobicity of the  
273 material [27]. The surface contact angles of the native starch and the modified starches were  
274 measured with a contact angle tester to determine the relative hydrophobicity, and the results are  
275 shown in Fig.4. As shown by the data presented in Fig.4, the initial contact angle of the native  
276 starch was only 37 ° and full absorption of water droplets required only 1.010 s. After the  
277 modification of in-situ solid phase polymerization, the initial contact angle was increased and the  
278 full absorption time of water droplets was prolonged for all grafted starches. The results suggested  
279 better hydrophobicity of the grafted starches compared to native starch, due to the replacement of  
280 the hydrophilic hydroxyl groups on the bamboo fiber with hydrophobic carbonyl groups. The  
281 contact angle and the time of full absorption varied for the three kinds of grafted starches. The  
282 LA-g-starch had the largest contact angle and the longest absorption time and the MA-g-starch  
283 had the smallest contact angle and the shortest absorption time, indicating that the hydrophobicity  
284 of LA-g-starch was the best and that of MA-g-starch was the worst. The hydrophobicity of the  
285 grafted starches was directly related to the number of hydrophobic groups grafted into the starch,  
286 and more hydrophobic groups resulted in better hydrophobicity. Thus, the measured contact angles  
287 were consistent with the grafting ratios.





288

289 **Fig.4 Initial surface contact angle for the native starch and grafted starches**

290 To further confirm that graft modification can improve the hydrophobic properties of native  
 291 starch, the water absorption of the materials was determined based on their relative weight change  
 292 after exposure to water. The results are shown in Table 2. After incubation of the samples in a wet  
 293 environment for 144 hours, the weight gain rate of the samples became stable, as saturation was  
 294 reached. The water absorption of the grafted starches was lower than that of native starch for the  
 295 144 hours of measurement. Again, the results indicated that reaction between the hydrophobic  
 296 monomer and native starch enhanced the hydrophobicity of the starch. Comparison of the water  
 297 absorption for the three kinds of grafted starches revealed that LA-g-starch was the lowest and  
 298 MA-g-starch was the highest. Thus, the LA-g-starch had the best hydrophobicity, and the  
 299 MA-g-starch had the worst. The results were in agreement with the contact angle test results.

300 **3.4 Molecular weight change of grafted starches**

301 As shown in Fig. 1, the graft copolymerization can increase the molecular weight of native  
 302 starch. To verify the feasibility of the in-situ solid polymerization reaction, native starch,  
 303 MAH-g-starch, LA-g-starch and MA-g-starch were characterized by gel permeation  
 304 chromatography (GPC) and the results are shown in Table 2.

305 **Table 2 water absorption change and molecular weight of native starch and grafted starches**

Starch species	Water absorption (%)						Molecular weight		
	24h	48h	72h	96h	120h	144h	$M_n$ (D)	$M_w$ (D)	DI
Native starch	20.175	22.679	24.649	26.680	27.556	27.584	$7.869 \times 10^4$	$4.325 \times 10^5$	5.496
MAH-g-starch	16.487	19.060	20.932	22.973	23.992	24.389	$8.422 \times 10^4$	$7.528 \times 10^5$	8.938
LA-g-starch	12.981	15.288	17.112	18.856	19.369	19.554	$1.726 \times 10^5$	$2.141 \times 10^6$	12.405
MA-g-starch	17.423	20.320	22.823	25.069	26.486	26.717	$8.014 \times 10^4$	$4.812 \times 10^5$	6.004

306

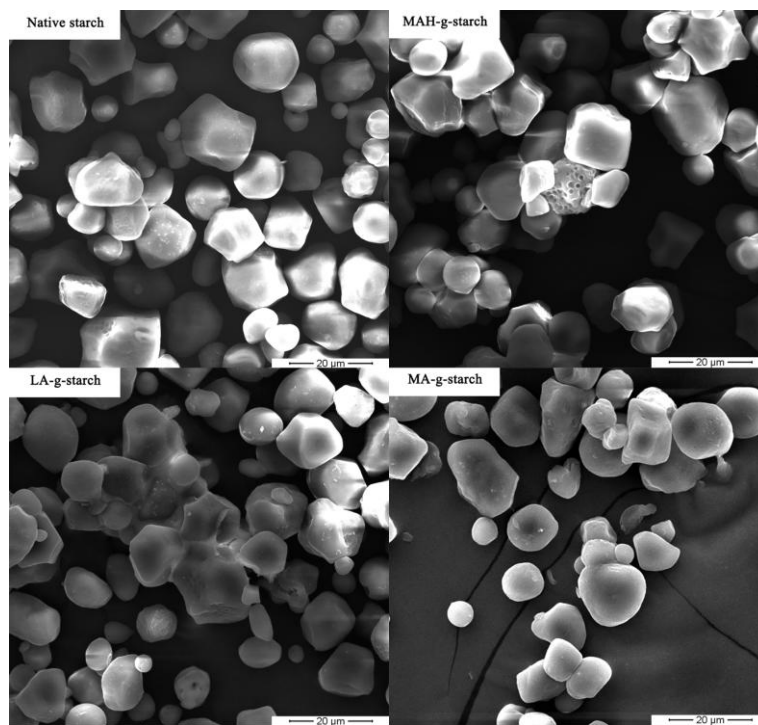
307 It can be seen from Table 2, the number-average molecular weight ( $M_n$ ) of native starch was  
 308  $7.869 \times 10^4$  D, the weight average molecular weight ( $M_w$ ) was  $4.325 \times 10^5$  D, and the distribution index  
 309 (DI) was 5.496. Compared with native starch, the  $M_n$  and  $M_w$  of grafted starches increased and the  
 310 DI increased also. It was also proved that the grafting monomers were successfully grafted onto  
 311 the starch molecular chain. However, the  $M_n$ ,  $M_w$  and DI of grafted starches obtained by different  
 312 grafting monomers was different. The  $M_n$  and  $M_w$  of from large to small was LA-g-starch,

313 MAH-g-starch, MA-g-starch. The molecular weight distribution index also showed the same trend.  
314 This phenomenon was closely related to the grafting ratio of grafted starches. In [Table 1](#), the  
315 grafting ratio of LA-g-starch was the largest, the polylactic acid molecular chain grafted on the  
316 starch molecular chain was the most. But the grafting ratio of MA-g-starch was only 0.57%, which  
317 leads to the minimum molecular weight and distribution index.

318 For polymers, viscosity was proportional to molecular weight. In order to further verify the  
319 effect of the in-situ solid phase polymerization on the molecular weight of modified starches, the  
320 pasting viscosity of the native starch and grafted starches were tested. The pasting viscosity of the  
321 native starch was 16500 mPa.s. Compared with the native starch, the pasting viscosity of all  
322 grafted starches were increased. The pasting viscosity of MAH-g-starch, LA-g-starch and  
323 MA-g-starch were 23600 mPa.s, 27100 mPa.s and 17200 mPa.s, respectively. It was proved that  
324 the molecular weight of starches increased after graft copolymerization. The pasting viscosity of  
325 LA-g-starch was the largest and MA-g-starch was the smallest, which indicated that the average  
326 molecular weight of LA-g-starch was the largest and that of MA-g-starch was the smallest. This  
327 also validates the results of the GPC test.

### 328 3.5 Morphology change of grafted starches

329 Scanning electron microscopy, in principle, was to use a very fine focused high-energy  
330 electron beam to scan the sample and stimulate a variety of physical information, by accepting,  
331 amplifying and displaying this information, the surface morphology of the test specimen was  
332 observed. The various samples of test materials were subjected to SEM analysis to determine the  
333 extent of any changes in surface morphology of the material as a result of the grafting reaction.



334

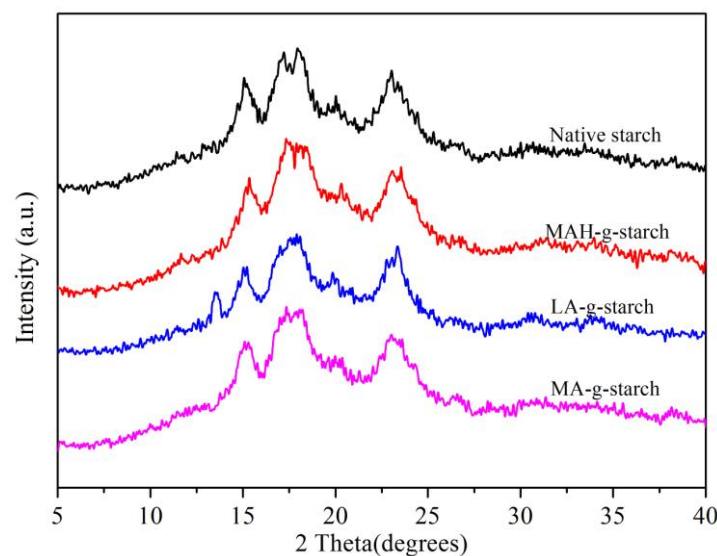
335 **Fig.5 SEM images of native starch and grafted starches**

336 [Fig.5](#) shows the SEM micrographs of the grafted starch, where it can be seen that the native  
337 starch granules were solid circles with smooth surface and edges. Comparison with the native  
338 starch, the in-situ solid phase polymerization did not destroy the granule structure of the starch.  
339 This may be because solid phase reaction process was conducted under anhydrous conditions, and

340 there was no starch gelatinization. There were morphological changes in the grafted starches, as  
341 the surface became rough and the granule surface was destroyed. This was because the graft  
342 polymer was grown on the starch granules, and the granules were bonded together. However, there  
343 was no obvious change in granule size, indicating that in-situ solid phase polymerization mainly  
344 occurred on the surface of the starch granule. The SEM micrographs showed that the surface  
345 roughness and bond degree of MAH-g-starch and LA-g-starch were more obvious, especially for  
346 the LA-g-starch. The results indicate that the surface roughness of the grafted starch was  
347 positively correlated with the grafting ratio.

### 348 3.6 Crystalline structure change of grafted starches

349 The FTIR, XPS, and SEM analysis of grafted starches all verified that a grafting reaction  
350 occurred as a result of the in-situ solid phase polymerization method. Therefore, it was  
351 reasonable to assume that the crystalline structure of the reactants had also changed. We next  
352 analyzed the crystalline structure of the native starch and the grafted starches to further verify  
353 this conclusion. The XRD method was used to determine if there was any change in the  
354 crystal structure of the native starch as a result of the grafting reaction, and the results are  
355 shown in Fig.6.



356

357

**Fig.6 XRD diffraction patterns of native starch and grafted starches**

358

359

360

361

362

363

364

365

366

367

368

369

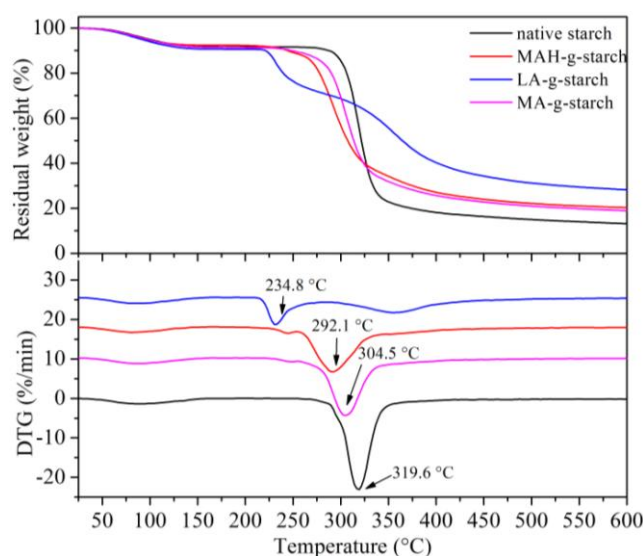
370

The XRD diffraction peaks for native starch were typical of an A-type crystalline structure, with  $2\theta$  values of  $15^\circ$ ,  $17^\circ$ ,  $18^\circ$  and  $23^\circ$  [28]. After the grafting reaction, the crystallization type of grafted starches did not change, suggesting that the reaction mainly occurred in the amorphous areas of the starch. The intensity of the XRD diffraction peaks in the hydrophobically modified starch was clearly weaker compared to those of the native starch. According to the report [29], it can be calculated that the degree of crystallinity of native starch was 27.93%, and after modification, the crystallinity of the grafted starches was reduced to varying degrees. This suggested that in-situ solid phase polymerization could destroy the crystalline structure of starch to some extent. In other words, the hydrogen bonds between molecules were weakened, thus the thermoplasticity of grafted starches increased [30]. This phenomenon was due to infiltration of the hydrophobic monomers into the crystalline area to destroy the hydrogen bonding between the molecules in this region. At the same time, the hydroxyl groups on the starch chain reacted with the hydrophobic monomers, and the molecular chains gradually grew and crosslinked, which

371 further destroyed the crystallinity of the starch. The decrease in the crystallinity of the grafted  
372 starches varied, as the MAH-g-starch decreased to 23.47%, LA-g-starch decreased to 22.29%, and  
373 MA-g-starch decreased to 24.69%. The grafting ratio of LA-g-starch was the highest and more  
374 hydroxyl groups on the chain of starch reacted, with the most serious destruction of hydrogen  
375 bonds. The grafting ratio of MA-g-starch was the lowest and the destruction of its crystalline  
376 structure was the smallest. More graft polymer molecular chains attached to the starch molecular  
377 chain resulted in a more loose structure.

### 378 3.7 Thermal performance analysis

379 The thermal behavior of the native starch and grafted starch were analyzed by TGA, and the  
380 results are shown in Fig.7. The thermogravimetric curves in Fig.7 show three stages at 50~120 °C,  
381 200~350 °C, and 400~600 °C. The first stage (50~120 °C) represented the evaporation of water  
382 from the starch. In the second stage (200~350 °C), native starch and grafted starches thermally  
383 decomposed, and the fastest rate of decomposition was observed in this stage. However, in the  
384 presence of the different hydrophobic monomers grafted on the starch, the rate of heat loss was  
385 also different. In the third stage (above 400 °C), the remaining material was decomposed to carbon  
386 by pyrolysis. The heat loss rate of the grafted starches was greater than that of native starch, and  
387 there was less decomposed residue. Comparing the residual weight, it appeared that the grafted  
388 starch materials had an increased weight loss rate (residual reduction), but the initial temperature  
389 for thermal decomposition and heat loss was reduced. This result also suggested an increase in the  
390 plasticity of the starch as a result of the grafting reaction. The XRD results showed that  
391 modification destroyed the starch crystallization and the density degree of the starch molecules  
392 decreased, so the grafted starch decomposed easily when heated. Of the grafted starch materials,  
393 the initial temperature of LA-g-starch was the lowest and the decomposition residual rate was the  
394 highest, and the MA-g-starch showed the opposite trends. The LA-g-starch was most easily  
395 decomposed, indicating the best thermoplasticity in the melting process. The most serious damage  
396 was evident for the crystalline structure of the LA-g-starch, and the MA-g-starch crystallinity was  
397 the lowest.



398

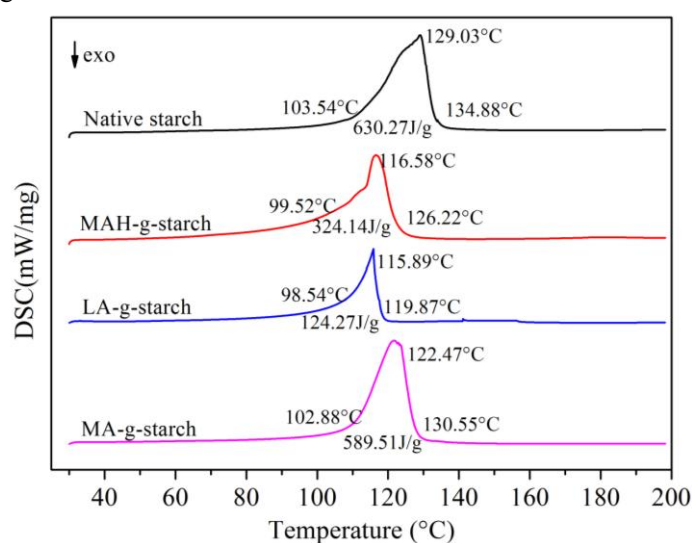
399 **Fig.7 TGA and DTG curves of native starch and grafted starches**

400 The DTG results in Fig.7 show a heat loss rate-accelerated peak for several kinds of starch  
401 that represents the maximum decomposition rate temperature. The maximum decomposition rate

402 temperature of the native starch was 319.6 °C, but the grafted starches showed obviously lower  
 403 values. This was due to the destruction of the crystalline structure of the starch by the modification  
 404 of the in-situ solid phase polymerization, reducing the decomposition temperature of the grafted  
 405 starches. The results agreed with the results of TG analysis, and the maximum decomposition rate  
 406 temperature of the LA-g-starch was the lowest and that of MA-g-starch was the highest.

### 407 3.8 Thermoplasticity change of grafted starches

408 DSC is a common method for researching melting properties [31]. The starch melting can  
 409 also be used to characterize the degree of difficulty for starch plasticization. By comparing the  
 410 DSC endothermic peak area, the change of melting enthalpy after grafting modification by  
 411 different monomers. The degree of gelatinization of native starch, MAH-g-starch, LA-g-starch and  
 412 MA-g-starch were tested by DSC, and the results are presented in Fig.8. The thermal transitions  
 413 temperature of the samples were defined as  $T_o$  (onset),  $T_p$  (peak) and  $T_c$  (conclusion), and the  
 414 enthalpy of melting was referred to as  $\Delta H$ .



415  
 416

**Fig.8 DSC curves of native starch and grafted starches**

417 As can see in Fig.8, native starch showed  $T_o$  and  $T_p$  between 103.54 and 134.88 °C,  $T_p$  was  
 418 129.03 °C, and  $\Delta H$  was 630.27J/g. After in-situ solid phase grafting modification of MAH, LA and  
 419 MA, the  $T_o$ ,  $T_p$ ,  $T_c$  of grafted starches all shifted to lower temperature, and  $\Delta H$  was decreased to  
 420 varying degrees. It was indicated that the grafted starches was easier to gelatinization and lower in  
 421 enthalpy of gelatinization. This was mainly attributable to the decrease of crystallinity and  
 422 intermolecular loosening after graft modification. There were differences in gelatinization  
 423 temperature and gelatinization enthalpy of three grafted starches. The all  $T_o$ ,  $T_p$ ,  $T_c$  and  $\Delta H$  of  
 424 LA-g-starch were the lowest, and MA-g-starch was the highest. The reason for this difference was  
 425 that the degree of crystallinity of the three kind of grafted starches varies with different grafting  
 426 ratio. At the same time, this indicates that LA-g-starch had the best thermoplasticity and MA-g-  
 427 starch was the worst.

### 428 4. Conclusion

429 This study demonstrated the successful preparation of three grafted starches using an in-situ  
 430 solid phase polymerization reaction. The grafting ratios of the MAH-g-starch, LA-g-starch, and  
 431 MA-g-starch were 6.50%, 12.45%, and 0.57%, respectively. The grafted reaction resulted from  
 432 replacement of the hydroxyl groups on D-anhydroglucose moieties of the starch with hydrophobic  
 433 carbonyl groups form the graft monomer, which resulted in improved hydrophobic characteristics



434 of the starch. With the influence of the grafting ratio, LA-g-starch had the best hydrophobic  
435 properties, and MA-g-starch had the worst. The  $M_n$ ,  $M_w$  and DI of LA-g-starch was the largest and  
436 MA-g-starch was the smallest. The surface of the grafted starches was covered with graft polymer,  
437 and the surface roughness and the bond degree of the MAH-g-starch and LA-g-starch were more  
438 obvious. The starch crystalline structure was destroyed by the grafting reaction, the degree of  
439 crystallinity was decreased, and the hydrogen bonding between the starch molecules was  
440 weakened, resulting in improved thermoplasticity in the grafted starches. For the degree of  
441 crystallinity of grafted starches, MAH-g-starch decreased to 23.47%, LA-g-starch was 22.29%,  
442 and MA-g-starch was 24.69%. The degree of thermoplasticity improvement from large to small  
443 was LA-g-starch, MAH-g-starch, and MA-g-starch.

444 The grafted starches produced by in-situ solid phase polymerization exhibited increased  
445 overall hydrophobicity with increased interface compatibility, allowed expanded application of  
446 thermoplastic starch and starch/plastic composites. This work comparing the influence of three  
447 grafting monomers on the grafting ratio and hydrophobic modification of starch provides  
448 reference data for the preparation of blended composites of starch and different polymers.

#### 449 Acknowledgments

450 This work was financially supported by the Key Laboratory of Bio-based Material Science &  
451 Technology (Northeast Forestry University), Ministry of Education (SWZCL2016-04), and the  
452 Scientific Research Project of Hunan Provincial Education Department (15C1428).

#### 453 References

- 454 [1] Ma X., Chang P.R., Yu J. Properties of biodegradable thermoplastic pea starch/carboxymethyl  
455 cellulose and pea starch/microcrystalline cellulose composites. *Carbohydr. Polym.* **2008**, *72*,  
456 369-375.
- 457 [2] Raquez J.M., Nabar Y., Srinivasan M., Shin B.Y., Narayan R., Dubois P. Maleated  
458 thermoplastic starch by reactive extrusion. *Carbohydr. Polym.* 2008, *74*, 159-169.
- 459 [3] Rodríguez-Castellanos W., Martínez-Bustos F., Jiménez-Arévalo O., González-Núñez R.,  
460 Rodríguez-González F.J., Ramsay B.A., Favis B.D. Rheological and thermal properties of  
461 thermoplastic starch with high glycerol content. *Carbohydr. Polym.* 2004, *58*, 139-147.
- 462 [4] Gross R.A., Kalra B. Biodegradable polymers for the environment. *Science*. 2002, *297*,  
463 803-807.
- 464 [5] Willett J.L. Mechanical properties of LDPE/granular starch composites. *J. Appl. Polym. Sci.*  
465 2005, *54*, 1685-1695.
- 466 [6] Wang X.L., Zhang Y.R., Wang Y.Z. Recent progress in starch-based polymeric materials. *Acta.*  
467 *Polym. Sin.* 2011, *28*, 24-37.
- 468 [7] Zuo Y.F., Gu J.Y., Yang L., Qiao Z.B., Tan H.Y., Zhang Y.F. Preparation and characterization of  
469 dry method esterified starch/polylactic acid composite materials. *Int. J. Biol. Macromol.* 2014,  
470 *64*, 174-180.
- 471 [8] Kaur B., Ariffin F., Bhat R., Karim A. Progress in starch modification in the last decade. *Food.*  
472 *Hydrocolloid.* 2012, *26*, 398-404.
- 473 [9] Xiong Z., Ma S.Q., Fan L.B., Tang Z.B., Zhang R.Y., Na H.N., Zhu J. Surface hydrophobic  
474 modification of starch with bio-based epoxy resins to fabricate high-performance polylactide  
475 composite materials. *Compos. Sci. Technol.* 2014, *94*, 16-22.
- 476 [10] Mani R., Bhattacharya M., Tang J. Functionalization of polyesters with maleic anhydride by  
477 reactive extrusion. *J. Polym. Sci. Polym. Chem.* 1999, *37*, 1693-1702.

- 478 [11] Shi D.A., Yang J.H., Yao Z.H., Wang Y., Huang H.L., Jing W., Yin J.H., Costa G.  
479 Functionalization of isotactic polypropylene with maleic anhydride by reactive extrusion:  
480 mechanism of melt grafting. *Polymer*. 2001, 42, 5549-5557.
- 481 [12] Xie F.W., Yu L., Liu H.S., Chen L. Starch modification using reactive extrusion.  
482 *Starch-Starke*. 2006, 58, 131-139.
- 483 [13] Sagar D.A., Merrill E.W. Properties of fatty-acid esters of starch. *J. Appl. Polym. Sci.* 1995, 58,  
484 1647-1656.
- 485 [14] Huang L., Xiao C.M., Chen B.X. A novel starch-based adsorbent for removing toxic Hg (II)  
486 and Pb (II) ions from aqueous solution. *J. Hazard. Mater.* 2011, 192, 832-836.
- 487 [15] Wootthikanokkhan J., Wongta N., Sombatsompop N., Kositchaiyong A., Wong-On J.,  
488 Isarankura na Ayutthaya S., Kaabuaathong N. Effect of blending conditions on mechanical,  
489 thermal, and rheological properties of plasticized poly (lactic acid)/maleated thermoplastic  
490 starch blends. *J. Appl. Polym. Sci.* 2012, 124, 1012-1019.
- 491 [16] Xing G.X., Zhang S.F., Ju B.Z., Yang J.Z. Microwave assisted Synthesis of Starch Maleate  
492 by Dry Method. *Starch-Starke*. 2006, 58, 464-467.
- 493 [17] Lukasiewicz M., Kowalsk S. Low power microwave - assisted enzymatic esterification of  
494 starch. *Starch-Starke*. 2012, 64, 188-197.
- 495 [18] Biswas A., Shogren R.L., Kim S., Willett J.L. Rapid preparation of starch maleate half-esters.  
496 *Carbohydr. Polym.* 2006, 64, 484-487.
- 497 [19] Olivato J.B., Grossmann M.V.E., Yamashita F., Eiras D., Pessan L.A. Citric acid and maleic  
498 anhydride as compatibilizers in starch/poly (butylene adipate-co-terephthalate) blends by  
499 one-step reactive extrusion. *Carbohydr. Polym.* 2012, 87, 2614-2618.
- 500 [20] Yu T., Jiang N., Li Y. Study on short ramie fiber/poly (lactic acid) composites compatibilized  
501 by maleic anhydride. *Compos. Part. A. Appl. S.* 2014, 64, 139-146.
- 502 [21] Ge X.C., Xu Y., Meng Y.Z., Li R.K.Y. Thermal and mechanical properties of biodegradable  
503 composites of poly (propylene carbonate) and starch-poly (methyl acrylate) graft copolymer.  
504 *Compos. Sci. technol.* 2005 65, 2219-2225.
- 505 [22] Sandhu, K.S., Singh, N. Some properties of corn starches II: Physicochemical, gelatinization,  
506 retrogradation, pasting and gel textural properties. *Food. Chem.* 2007, 101, 1499-1507.
- 507 [23] Zuo Y.F., Liu W.J., Xiao J.H., Zhao X., Zhu Y., Wu Y.Q. (2017). Preparation and  
508 characterization of dialdehyde starch by one-step acid hydrolysis and oxidation. *International*  
509 *Journal of Biological Macromolecules*, 103, 1257-1264.
- 510 [24] Zuo Y.F., Gu J.Y., Yan, L., Qiao Z.B., Tan H.Y., Zhang Y.H. Synthesis and characterization of  
511 maleic anhydride esterified corn starch by the dry method. *Int. J. Biol. Macromol.* 2013, 62,  
512 241-247.
- 513 [25] Dontulwar J.R., Borikar D.K., Gogte B.B. An esteric polymer synthesis and its  
514 characterization using starch, glycerol and maleic anhydride as precursor. *Carbohydr. Polym.*  
515 2006, 65, 207-210.
- 516 [26] Ma X.F., Chang P.R., Yu J.G., Wang N. Preparation and properties of biodegradable poly  
517 (propylene carbonate)/thermoplastic dried starch composites. *Carbohydr. Polym.* 2008, 71,  
518 229-234.
- 519 [27] Zeng J.B., Jiao L., Li Y.D., Srinivasan M., Li T., Wang Y.Z. Bio-based blends of starch and  
520 poly (butylene succinate)with improved miscibility, mechanical properties, and reduced  
521 water absorption. *Carbohydr. Polym.* 2011, 83, 762-768.

- 522 [28] Zuo Y.F., Gu J.Y., Tan H.Y., Qiao Z.B., Xie Y.H., Zhang Y.H. The characterization of granule  
523 structural changes in acid-thinning starches by new methods and its effect on other properties.  
524 *J. Adhes. Sci. Technol.* 2014, 28, 479-489.
- 525 [29] Singh V., Ali S.Z, Somashekar R., Mukherjee P.S. Nature of crystallinity in native and acid  
526 modified starches. *Int. J. Food. Prop.* 2006, 9, 845-854.
- 527 [30] Jiang W.B., Qiao X.Y., Tang Z.Z., Sun K. Preparation and properties of thermoplastic  
528 acetylated starch. *Acta. Polymer. Sin.* 2006, 23, 97-101.
- 529 [31] Maaruf A.G, Che Man Y.B., Asbi B.A., Junainah A.H., Kennedy J.F. Effect of water content  
530 on the gelatinisation temperature of sago starch. *Carbohydr. Polym.* 2001, 46, 331-337.